Journal of
Ceramic Science
and Technology

Thermography and Complementary Measurements as Tools to Detect Micro-Irregularities in Electronic Components

S. Röhrig[1, 2], I. Petschenig[1, 2], R. Bermejo[*1], M. Hofstätter[1], F. Aldrian[3], R. Danzer[1], P. Supancic[1, 2]

[1]Institut für Struktur- und Funktionskeramik, Montanuniversitaet Leoben, Austria
[2]Materials Center Leoben Forschung GmbH, Leoben, Austria
[3]EPCOS OHG, Deutschlandsberg, Austria

Abstract

In many ceramic components for electrical applications, small defects in the microstructure may cause an anomalous current flow. Especially in components exhibiting nonlinear electro-thermal properties, such as varistors, positive (PTC) or negative (NTC) temperature coefficient resistors, inhomogeneities lead to high concentrations of current and localized heat generation owing to positive feedback effects. While the integral behaviour of those components is largely unaffected by these defects, the local load at these hot spot regions is extremely high and can even lead to the complete failure of the device. In this work, microanalytical tools are combined to identify the location and type of defects that may cause leakage currents, overheating or other reasons for inhomogeneous current distributions in functional ceramic components. Lock-in thermography is used to localize dominating current paths. This is even possible if the heat sources are in the micrometer range or smaller. Additionally, microsectioning techniques (e.g. Focused Ion Beam) are utilized to expose such regions in order to investigate features of the microstructure and causes for the enhanced current flows. Examples are shown with PTC resistor components as well as Low-Temperature Co-fired Ceramic (LTCC)-based modules.

Keywords: Electroceramics, PTC, LTCC, inhomogeneities, microthermography, focused ion beam

I. Introduction

In microelectronic components, small irregularities in the microstructure may cause an unexpected flow of the current which may in turn disturb the functionality of the device. In components exhibiting nonlinear behaviour, such as varistors, positive temperature coefficient (PTC) or negative temperature coefficient (NTC) resistors, such irregularities may cause a high local concentration of current and – as a consequence – local heat generation. This can even cause the complete failure of the device. In dielectric components, such as Low-Temperature Co-fired Ceramic (LTCC) devices, some unintended leakage current can be present, e.g. caused by microcracks, which can also impair the functionality of the component.

In order to guarantee reliable functioning of the component, defects must not exceed certain thresholds in respect of size, shape and type. This is not easy to guarantee, because defects are commonly introduced during processing. Therefore, to ensure a component's minimum service life, proof testing (overload testing) of components is commonly applied [1–4]. In such tests, the component is loaded up to a mechanical stress higher than the service stress for which the component has been designed. As a result, all components containing equal or larger flaws as those corresponding to the proof stress are destroyed. However, a common problem in proof testing is that the in-service stress fields of components cannot be easily simulated in a test. For example, the stress fields caused by temperature changes or by contact loading can hardly be reproduced in simple mechanical tests. In such cases, large regions in the component may be subjected to a proof stress that is too high while other parts are subjected to stress that is too low. The first condition increases the rejection rate and the second condition only reduces the failure probability, but some in-service failures are still possible. Indeed both outcomes are undesirable.

Non-destructive evaluation methods (NDE) such as radioscopic testing and x-ray computer tomography (CT) are often used owing to their capability to visualize inner structures of the objects under investigation. They can be applied to numerous materials. For example, CT is well-established in the foundry industry for identifying internal casting defects such as pores, cavities or inclusions [5]. But up to now the method has not been commonly used for the detection of defects in advanced ceramics, because their spatial resolution is too low. E.g. when advanced microfocus x-ray-devices are used, the resolution is in the range of a few µm. Defects with sizes in this range or smaller cannot be detected with these devices. Closed cracks might also be undetectable, because the method is based on different attenuation of the x-rays caused by differences in the mass density, element distribution owing to different phases or

*   Corresponding author: raul.bermejo@unileoben.ac.at

materials. Therefore, the thickness of the specimen and experimental settings such as the focal spot size, detector pixel size or the distance between the source and the detector can limit the resolution to a few μm.

A different approach suited for some functional ceramics is based on thermographic analyses, aiming to detect the thermal response at the surface of components caused by an electrical excitation. The application of an electrical voltage to the electrically contacted specimen results in a specific electrical field distribution, which depends on the component's geometry and the material's properties. If a current is led through a component, Joule heating occurs. The local specific Joule heating rate p is given by:

$$p = \varrho\, j^2 \qquad (1)$$

where ϱ is the resistivity and j the current density. The temperature field induced at the surface of the component is strongly affected by the heat generation, and also by the design of the component (i.e. geometry, materials) and the thermal environment (i.e. cooling condition). Note that thermography does not measure the temperature distribution at the surface directly but the infrared radiation (IR) field, which is affected by the surface conditions and the emission coefficients of the materials. Therefore, the interpretation of the measurements is often not clear and unique. For quantitative analysis, modelling of the test is indispensable, especially if the effect of defects has to be extracted out of the data. Only in some particular cases is the expected temperature and IR field nearly constant or slowly varying, so that inhomogeneities can be easily detected. For example, the observation of localized cold or hot spots on a homogeneous surface during a heating process or in a steady-state condition is a clear indication of electrothermal defects ("standard thermography" [6]).

When the spatial temperature difference is too small or dominated by noise, "Lock-in thermography" is employed [7, 8]. Here, the specimen is excited by means of AC voltage and the thermal response is analysed for each pixel (i.e. for every location on the surface) in respect of the exciting frequency. The obtained amplitude and phase shift of the temperature variation provide information on the intensity of the local heat generation and the actual depth of the heat source under the surface. Successful applications to ceramic materials can be found for instance in varistor components [9–11].

To demonstrate the usefulness of thermography for detecting defects in microsystems, two ceramic components (one conductive and one dielectric) have been analysed in this work using standard and lock-in thermography, respectively. Samples were provided by the company EPCOS OHG (TDK Corporation), Deutschlandsberg, Austria. Standard thermography is used to reveal defects at the surface of PTC components. Lock-in thermography is employed to localize leakage current paths in LTCCs, which may occur at internal regions of the components. This is even possible if the heat sources are in the micrometer range. Additionally, complementary tools such as micro-sectioning techniques (e.g. Focused Ion Beam) are utilized to expose such regions and thus better understand the source of failure.

II. Methods

Over the last years, thermography has become a well-established investigation technique for non-destructive testing (NDT) of materials and devices. Especially electronic components are at the focus of interest, because electric inhomogeneities, failures or leakage paths have a direct impact on the local heat generation and in this way on the temperature distribution in the sample. The temperature distribution can be measured with thermography because every body radiates a heat flux, q, following the Stefan-Boltzmann law

$$q = \varepsilon(\lambda, a \dots)\sigma_{SB} T^4 \qquad (2)$$

with the temperature T and the Stefan-Boltzmann constant, σ_{SB}. ε is the emissivity and therefore a material constant, which may dependent on the wavelength, λ, of the emitted light, on the radiation angle, a, and/or other parameters. For example, the emissivity decreases with an increasing radiation angle. From this, it follows that the temperature of a cylindrical sample can appear colder at the border compared to at the centre, as will be shown in the next section.

Generally speaking, thermographic NDT can be divided into two groups: active and passive thermography, depending on how heat is generated in the specimen under investigation. In our exemplary cases, heat is induced electrically by the Joule heating effect (i.e. active thermography). Active thermography can be further divided into steady state and transient, the latter including pulsed and lock-in thermography. The first example will demonstrate the possibilities of pulsed thermography: the sample is heated as the result of a constant voltage. An analysis of the transient warming behaviour of the surface allows the investigation of features within solid objects [12–15]. The second example utilizes lock-in thermography. A sinusoidal voltage with an amplitude offset for unipolar excitation is applied to the specimen. After the decay of initial transients, the corresponding temperature field on the surface becomes periodic. Fourier analysis of the resulting temporal signal gives information about the size and depth of the defect. The big advantage of lock-in thermography is that the spatial resolution can be strongly enhanced, because it depends on the lock-in frequency f_{LI} by $1/\sqrt{f_{LI}}$. On the flip side, an increase of the lock-in frequency reduces the temperature modulation amplitude and thereby the signal quality. For an optimal measurement, a trade-off between these two competing effect has to be accepted [7, 8, 16, 17].

(1) Standard pulsed thermography on PTC samples

To detect possible inhomogeneities at the surface of PTC components, standard thermography was used. PTC disc-like specimens of 20 mm diameter and 5 mm thickness were clamped between two fixtures (see Fig. 1), which were excited with a DC-voltage of 230 V. The temperature distribution at the lateral surface of the PTC-disc was measured with an infrared camera (Cedip Flir JADE MW3), located in front of the disc on a rail track (see Fig. 1). The camera has a 320 x 240 pixel InSb focal plane array to capture radiation with a wavelength in the range of 3 μm to 5 μm. The image acquisition rate was set to 50 Hz.
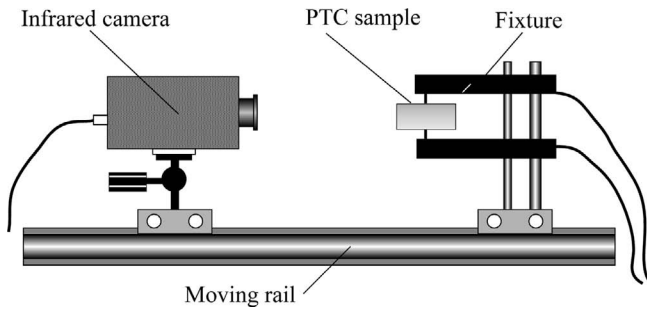
Fig. 1: Schematic of an IR camera mounted on a rail track in front of a PTC disc, clamped between two fixtures excited by a DC voltage of 230 V.

(2) Lock-in thermography on LTCC samples

To visualize and localize internal leakage current paths in LTCC modules, which cannot be accurately detected with standard thermography, lock-in thermography was employed. Plate-like LTCC sample modules that showed a relevant leakage current (at selected terminations) were contacted by means of two metallic needles, using a micro-manipulator (Model The Micromanipulator Co. No.: 2550) under a standard stereo-microscope (see Fig. 2).
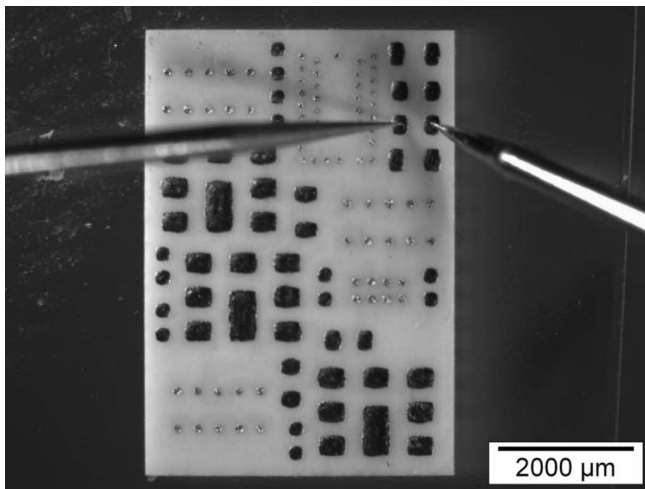

Fig. 2: LTCC module contacted with two metallic needles at two surface terminations.

This setup was positioned in front of the infrared camera, as used in Section II(1) for the PTC-sample (see Fig. 1). The image acquisition rate was set to 140 Hz. A sinusoidal voltage with an amplitude of a few volts and a frequency of 10 Hz was applied to the needles (function generator: Tektronix AFG 3000 and amplifier: NF HAS 4051). A series of 250 images (≈2 s) was taken and analysed pixel-by-pixel by means of Fourier transformation in respect of the base excitation frequency and its first harmonic. Note that since the electrical power is proportional to the square of the voltage, even a perfect sinusoidal voltage signal results in a power profile including harmonics in respect of the base excitation frequency.

(3) Cross-sectioning combining SEM and FIB

In order to identify particular locations of interest inside the samples analysed (e.g. pores, cracks, metallic particles, etc.) cross-sectioning, followed by fine polishing

of embedded specimens, was performed. Plate-like specimens were first embedded in an acrylic resin, with the cross-section facing upwards. A combination of grinding and fine polishing (down to 1 µm diamond paste) together with visual examinations using a light microscope (Olympus BX50, Tokyo, Japan) was carried out, aiming to reveal the region of interest. Further, in order to detect the possible internal feature responsible for the (inhomogeneous) "thermographic" response, Focused Ion Beam (FIB) equipment was utilized with an Auriga Cross-Beam workstation (Carl Zeiss, Oberkochen, Germany). The FIB gun consisted of a Ga-ion Cobra-FIB column (Orsay Physics, Fuveau, France) operating at high current with a nominal resolution of 2.5 nm. Typical FIB times were ~30 s per milling step. The FIB-columns were arranged within an angle of 54 ° to the electron column, which permitted direct observation within the Scanning Electron Microscope (SEM). The combination of a SEM with field emission gun and a gallium ion column allowed for high-resolution imaging.
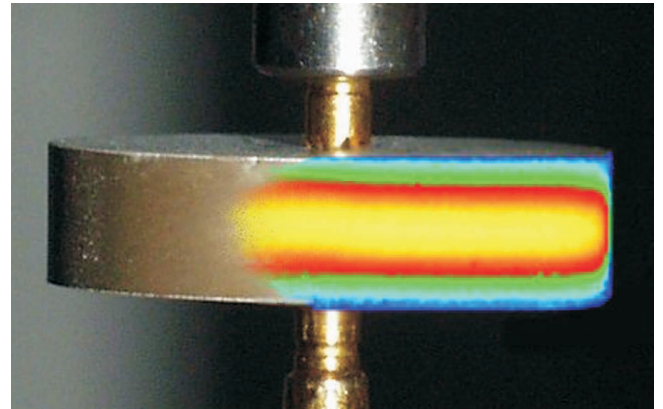

Fig. 3: Schematic of an overlay of a thermographic observed temperature field (colour-coded image on the right side) on a cylindrical PTC element, connected by two metallic electrodes.

III. Results and Discussion

(1) Active-component (PTC resistor)

PTC resistors exhibit an exponential increase of the electrical resistance with temperature in a given temperature range. Within a change of a few tens of K, a resistance change of typically 4 to 7 orders of magnitude can be induced. This behaviour is caused by the ferroelectric phase transition of the $BaTiO_3$-based material [18, 19]. Owing to this peculiar property, PTC elements are widely used as self-regulating heating elements, motor start elements or as self-resetting overcurrent protectors. In addition to active applications, PTC elements are also used as temperature and fluid level sensors (i.e. passive application). Active applications are characterized by applying a relatively high voltage, so that the Joule heating is able to induce a significant temperature change, typically above the phase transition temperature. The transient temperature change can be observed directly with a thermo-camera, as shown in Fig. 3; a cylindrical PTC component is driven by a 230 V AC source, while the temperature field at the cylinder barrel is recorded. Owing to the design of the component and the thermal boundary conditions, the

temperature maximum is located at the midplane of the component [20]. The recorded temperature field in Fig. 3 validates this expectation, since all observed features can be explained by a model based on an homogeneous PTC component.
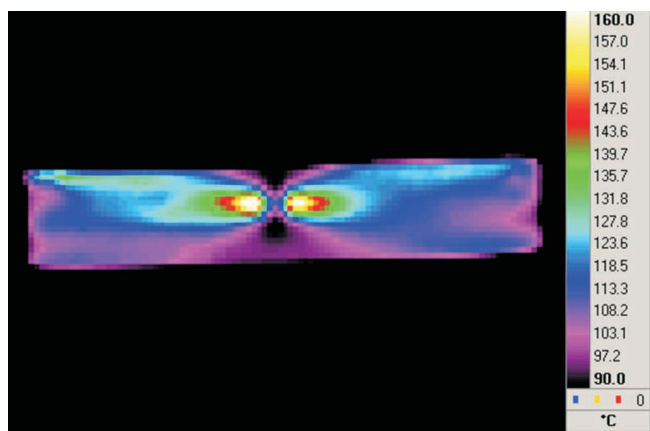

Fig. 4: Thermographic image of the surface of a PTC element during a switching process, showing an electrical (highly resistive) defect at the surface in the central region (cold spot).

A different thermographic image of a PTC component during a switching process is shown in Fig. 4. In this case, a cold spot is observed in the central region of the component, surrounded by two hot zones. A light microscopic analysis of the PTC disc reveals a microstructural defect at the surface of the component (see Fig. 5). Obviously, a highly resistive contamination leads to a cold spot at the defect position. On the other hand, the electrical current is squeezed out from the defect's region leading to a current concentration in the surroundings, i.e. left and right in respect of the current direction. Also this hypothesis can be validated by modelling the process with a highly resistive defect. Finally, this component has been tested with higher voltage to check whether this kind of defect is crucial under proof test conditions. As a consequence, the part failed during this test by fracturing into two parts (see Fig. 6). The failure was caused by the thermal mismatch of the cold spot zone within the surrounding hot region. The tensile-stressed electrical defect acted as fracture origin of the propagating crack, as depicted by arrows in Fig. 6. The fracture runs from the defect towards the inner part of the cylinder, causing catastrophic failure.
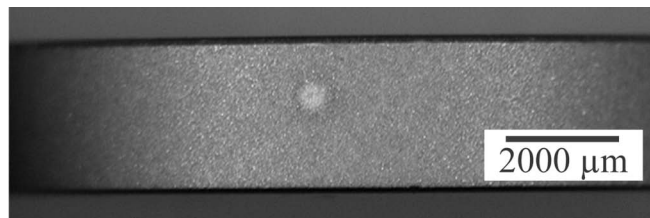

Fig. 5: Light microscopic image of the surface of the PTC element analysed in Fig. 4. A microstructural defect with different colour compared to standard PTC material can be found at the cylinder barrel (the yellowish colour indicates a highly resistive property).

(2) LTCC module with leakage current

Some special electrical circuit boards are made of ceramics instead of polymers. Actually metallic strip lines (electrodes) are embedded in the ceramic component, which

have to be sintered together. The use of a ceramic matrix is advantageous in terms of stiffness, small thermal expansion, small dielectric loss factors and stability at elevated temperatures [21]. Neighbouring metallic paths are separated by the ceramic providing an isolating resistance in the $T\Omega$ range, up to high electric field strength. Therefore no measurable current is induced by applying a DC voltage between separated contact pads.
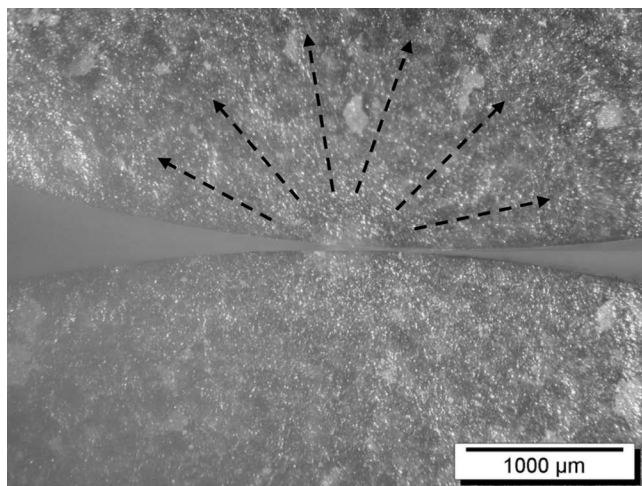

Fig. 6: Fracture surface of the same PTC element as shown in Fig. 4 and 5. The thermographically and optically detected surface defect is the fracture origin in the electric proof test. The fracture runs from the defect towards the inner part of the cylinder, as depicted by arrows, causing catastrophic failure.

In order to investigate the performance limits of the module, some overload tests in wet atmosphere at elevated temperature can be performed. In some cases, this may lead to small leakage currents, which can be found between selected strip lines. Thermographic methods can be used to localize the position of the leakage current in the component. However, in many cases the induced temperature change is in the range of a few mK, so that the hot spot cannot be directly recognized due to the measurement scatter. The use of the so-called lock-in technique enhances the temporal resolution significantly. The component is driven by a periodic voltage signal with a given frequency (for example by a sinusoidal voltage profile) and the temperature response is recorded after some initial transients with a sampling rate higher than the excitation frequency. Fourier analysis of the set of images in respect of time at each position reveals the regions that are affected by the electrical excitation: in steady-state condition the temperature field oscillates at the same frequency as the driving voltage. The higher the amplitude of the corresponding Fourier component is, the stronger is the heating effect at the investigated position. In Fig. 7 an amplitude image is shown as overlay on a sample LTCC module that has been subjected to harsh loading conditions. The phase shift between excitation and temperature response corresponds to a temporal delay, which is a measure of the depth of the heat source under the surface (i.e. defect with leakage current). This information can be used to expose the microstructure with the leakage current: after the component is embedded in epoxy resin, successive grinding steps have to be performed so that the phase shift of the thermographic lock-

in signal reduces to zero and the heat source appears at the specimen's surface.
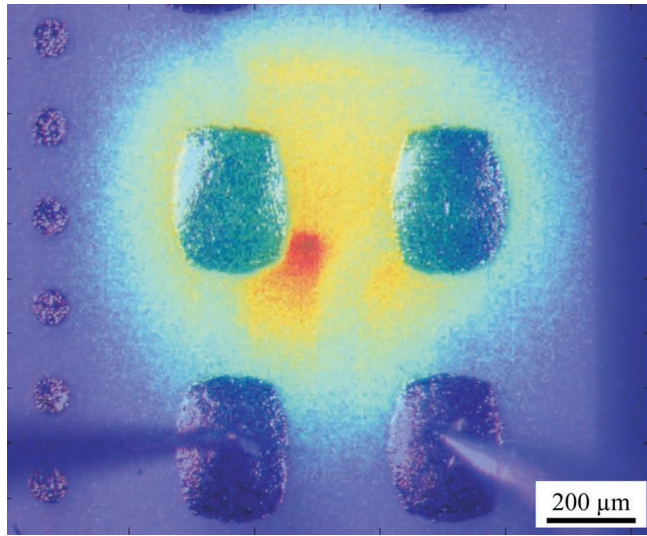

Fig. 7: Overlay of an amplitude image obtained by a Fourier analysis of a set of thermographic images during a periodic excitation of a LTCC module with an internal leakage current path (top plane view).

To investigate the origin of the leakage current in the microstructure, a local cut with a FIB was produced which can be monitored with scanning electron microscopy. In the case of the demonstrated example, the leakage current region is located between a neighbouring pair of inner electrode planes, see Fig. 8. The insert shows the SEM image of the hot spot zone. Actually, some microcracks are found, partly filled by electrode material, which has migrated into the cracks during the overload test. This feature is responsible for the significantly reduced electrical resistance. While lock-in thermography in combination with an IR microscope was able to detect this defect on the μm range, tomography failed to detect this feature.
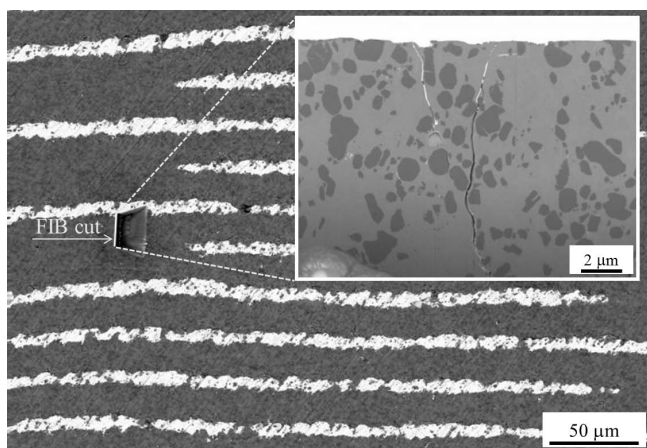

Fig. 8: Cross-section exposing a leakage current zone in a LTCC module by successive grinding and checking the phase shift of the thermographic lock-in signal. The inset shows a SEM image of the defect after preparing a FIB cut: Cracks partly filled with metals are visible.

IV. Conclusions

It has been demonstrated that thermography can detect electrothermal defects in electroceramic components. In some cases, the diagnosis has to be supported by simulation tools to distinguish between different causes for cold and hot spots. If the change in temperature is significant, the relevant information can be extracted directly from the recorded thermographic images. This has been demonstrated based on the example of active switching of a PTC component. On the other hand, if the electro-thermally induced temperature change is too small, the application of lock-in thermography can drastically enhance the thermal resolution. An example has been shown with the detection of a leakage current inside a complex-shaped LTCC module. Even though the induced temperature oscillation was as small as a few mK, the defect was located and exposed by successive grinding steps together with the phase information of the lock-in signal. While these results were obtained in laboratory conditions, the technical preconditions are (nearly) fulfilled to set up thermography as a tool for materials/components testing on a production line as it is already used to test poor contacts, unbalanced loads or other overheating causes of electrical devices.

References

[1] Davidge, R.W.: Mechanical behaviour of ceramics. Cambridge University Press, Cambridge, 1979.

[2] Soma, T., Ishida, Y., Matsui, M., Oda, I.: Ceramic component design for assuring long-term durability, *Adv. Ceram. Mater.*, **2**, 809–812, (1987).

[3] Morrell, R.: Handbook of properties of technical & engineering ceramics, Part 1: An introduction for the engineer and designer. Her Majesty's Stationery Office, London, 1989.

[4] Munz, D., Fett, T.: Ceramics. Mechanical properties, failure behaviour, materials selection. Springer, Berlin, 1999.

[5] Geier, G., Rosc, J., Hadwiger, M., Fritz, L., Habe, D., Pabel, T., Schumacher, P.: Assessing casting quality using computed tomography with advanced visualization techniques. In Shape Casting: 3rd International Symposium. 2009.

[6] Buse, G., Wu, D., Karpen, W.: Thermal wave imaging with phase sensitive modulated thermography, *J. Appl. Phys.*, **71**, 3962–3965, (1992).

[7] Breitenstein, O., Langenkamp, M., Altmann, F., Katzer, D., Lindner, A., Eggers, H.: Microscopic lock-in thermography investigation of leakage sites in integrated circuits, *Rev. Sci. Instrum.*, **71**, 4155–4160, (2000).

[8] Breitenstein, O., Watrta, W., Langenkamp, M.: Lock-in thermography: Basics and use for evaluating electronic devices and materials. 2nd ed. Springer, 2010.

[9] Hofstätter, M., Nevosad, A., Teichert, C., Supancic, P., Danzer, R.: Voltage polarity dependent current paths through polycrystalline ZnO varistors, *J. Eur. Ceram. Soc.*, **33**, 3473–3476, (2013).

10 Hofstätter, M., Raidl, N., Sartory, B., Supancic, P.: Nonlinear lock-in infrared Microscopy: A complementary investigation technique for the analysis of functional electroceramic components, *Microsc. Microanal.,* **21**, [5], 1145 – 1152, (2015).

11 Raidl, N., Supancic, P., Danzer, R., Hofstätter, M.: Piezotronically modified double Schottky barriers in ZnO varistors, *Adv. Mater.,* **27**, [12], 2031 – 2035, (2015).

12 Cielo, P., Maldague, X., Déom, A.A., Lewak, R.: Thermographic non-destructive evaluation of industrial materials and structures, *Mater. Eval.,* **45**, 452 – 460, (1987).

13 Maldague, X., Marinetti, S.: Pulse phase infrared thermography, *J. Appl. Phys.,* **79**, 2694 – 2698, (1996).

14 Giorleo, G., Meola, C.: Location and geometry of defects in composite laminates from infrared images, *ASM Int. J. Magn. Eng. Perf.,* **7**, 367 – 374, (1998).

15 Oswald-Tranta, B.: Time-resolved evaluation of inductive pulse heating measurements, *Quant. Infrared Thermogr. J.,* **6**, [1], 3 – 19, (2009).

16 Sakagami, T., Kubo, S.: Applications of pulse heating thermography and lock-in thermography to quantitative nondestructive evaluations., *Infrared Phys. Technol.,* **43**, [211 – 218], (2002).

17 Meole, C., Carlomagno, G.M., Squillace, A., Vitiello, A.: Nondestructive evaluation of aerospace materials with lock-in thermography, *Eng. Fail. Anal.,* **13**. 380 – 388, (2006).

18 Heywang, W.: Semiconducting barium titanate, *Mater. Sci.,* **6**, 1214 – 1224, (1971).

19 Moulson, A.J., Herbert, J.M.: Electroceramics. Chapman & Hall, London, Weinheim, New York, Tokyo, Melbourne, Madras, 1997.

20 Supancic, P.: Mechanical stability of $BaTiO_3$-based PTC thermistor Components: experimental investigations and theoretical modelling, *J. Eur. Ceram. Soc.,* **20**, [12], 2009 – 2024, (2000).

21 Imanaka, Y.: Multilayered low temperature cofired ceramics (LTCC) technology. In, New York, NY 10013, USA, 2005.